

Failure Detection by Pilots during Automatic Landing: Models and Experiments

Eliezer G. Gai*

C. S. Draper Laboratory, Cambridge, Mass.

and

Renwick E. Curry†

Massachusetts Institute of Technology, Cambridge, Mass.

A model is proposed to describe the pilot as a monitor of automatic landing systems. The failures treated are equivalent to the addition of a dynamic change in the mean of the observation process. The failure detection model of the pilot consists of two stages: a linear estimator (Kalman filter) and a decision mechanism based on sequential analysis. The filter equations are derived from a simplified version of the linearized dynamics of the airplane and the control loop. The perceptual observation noise is modified to include the effects of allocation of attention among the several instruments. The final result is a simple model consisting of a high-pass filter to produce the observation residuals and a decision function which is a pure integration of the residuals minus a bias term.

The dynamics of a Boeing 707 were used to simulate the fully coupled final approach in a fixed-base simulator which included failures in the airspeed and glideslope indicators. Observers monitored the approaches and detected the failures; their performance was compared with the predictions of the model with good agreement between the experimental and the model.

Introduction

THE introduction of the "all weather" automatic landing system changes the role of the pilot during landing. Under normal conditions, the pilot is not in the control loop, but his main task is to monitor the proper operation of the automatic system. This, of course, shifts his role from manual controller to decision maker. This paper considers the task of modeling the pilot as a monitor of the automatic system using the information available from conventional instrument sources. Mode progress and failure annunciators are not considered in this first step of modeling the pilot, since a basic model of the analog-information processing does not exist for this task. Moreover, the pilot is likely to use the conventional instruments alone to assess the validity of any alarm indications; the addition of the annunciators can very likely be represented as a change in the threshold of the model that is proposed.

The problem of modeling the pilot as a controller has been addressed by several researchers, and satisfactory models exist using classical control theory^{1,2} or optimal control theory.³ Models for the pilot as a failure detector have only recently been addressed,⁴ and some conjecture has been suggested.⁵

The development of a model for the human observer in the failure detection task is based on several fundamental hypotheses. In developing these hypotheses, we have drawn on the previous work in manual control, which in itself has established a set of working hypotheses. These hypotheses, developed by McRuer and his colleagues,⁶ are repeated in the following.

1) To accomplish guidance and control function, such as flying a desired track in the presence of disturbances,

maintaining precision control (as in formations and refueling), flying intercepts or approaches, etc., the human pilot sets up a variety of closed-loops about the aircraft, which, by itself, could not otherwise accomplish these tasks. In control system engineering terms, his control actions are functions of desired and actual aircraft motions.

2) To be satisfactory, these closed-loop systems, comprising both animate and inanimate components, must share certain qualitative dynamic features of "good" closed-loop systems of solely inanimate nature. As the adaptive means to accomplish this end, the pilot must make up for any dynamic deficiencies of the aircraft by appropriate adjustments to his dynamic properties. (Here the "aircraft" includes the display and controls.)

3) There is a cost to this adjustment—in workload induced stress, in concentration of pilot faculties, and in reduced potential for coping with the unexpected. This cost can also be traded for the cost of automatic controls. In making this tradeoff, one may allocate part of the task to manual and part to automatic control.

The field of modeling human failure detection has an infinitesimal data base relative to the field of manual control. Thus, the following is offered as a tentative set of hypotheses to be revised as indicated by future experimentation.

1) To accomplish the system monitoring functions such as monitoring the state of the aircraft, its various subsystems (including instrumentation), the observer sets up a variety of models about the aircraft and its performance based on his past experience.

2) To be satisfactory, these monitoring systems, comprising both animate and inanimate components, must share certain of the qualitative dynamic features of "good" failure detection systems of the solely inanimate nature. As the adaptive means to accomplish this end, the pilot must make up for any dynamic deficiency of the information displayed by appropriate adjustments of his dynamic information processing.

3) There is a cost to this adjustment—in workload induced stress, in concentration of pilot faculties, and in reduced potential for coping with the unexpected. This cost can also be

Received July 30, 1975; revision received April 30, 1976.

Index categories: Aircraft Crew Training; Aircraft Handling, Stability, and Control; Safety.

*Staff Engineer.

†Associate Professor, Department of Aeronautics and Astronautics.

traded for the cost of automatic monitoring systems. In making this tradeoff, one may allocate part of the task to the human and part to automatic failure detection systems.

In this paper, a model of a pilot as a monitor of instruments failures (dynamic biases) is proposed and applied to an automatic landing. The model consists of two states: a linear estimator and a decision mechanism. The linear estimator is the Kalman filter which is similar to that used in the optimal controller models with the measurement residuals, rather than the estimates, as outputs. The decision mechanism is based on sequential analysis⁷ modified for the special case of failure detection.⁸ An experiment was conducted to validate the proposed model; observers monitored instrument failures in simulated automatic ILS approaches in a fixed-base jet transport cockpit. The results of this experiment are then compared to the prediction of the model.

Problem Statement and Simplification

A functional block diagram of the failure detection paradigm is shown in Fig. 1. The failures considered in the analysis are restricted to the class of output-additive time functions which alter the mean of the observed process. This type of failure can occur, for example, because of electrical and/or mechanical biases within the sensor or instrumentation signal processing. As in all single-instrument failures, it is manifested by an indication which is inconsistent with other readings, whereas actuator and/or sensor failures used for automatic flight control exhibit consistent readings of an abnormal maneuver.

A basic assumption in the structure of the first stage of the human detection model (the estimation stage) is that the dynamical characteristics of the system that produces the input signals are known by the observer. Therefore, before modeling the failure detection system in detail, the representation of the airplane dynamics and control loops, by the pilot (his internal model) will be discussed.

The true airplane dynamics, when angular accelerations are neglected, can be defined by nine first-order nonlinear differential equations. Two decoupled autopilots are used to regulate the vertical error between the aircraft position and the glideslope beam, and the horizontal (angular) error between aircraft position and localizer beam. In addition, a third control loop regulates the aircraft speed. This configuration was used in the simulation that automatically landed the Boeing 707 dynamics used in our experiments.⁹

Since the pilot is outside the control loop, his inputs consist only of the displayed variables on his instrument panel. If the control system is designed properly, these displays will show nominal values with variation due to outside perturbations. It seems reasonable to assume that the internal representation of the pilot will be a linearized version of the automatic system around the nominal values. In addition, the longitudinal and lateral dynamics are assumed to be decoupled in this representation. The block diagrams of the three control loops are shown in Fig. 2, where the basic configuration was taken from Ref. 10. The three closed loop transfer functions are given by

$$\frac{\delta u}{\delta u_n} = \frac{10(s+0.1)}{(s+8.8)(s+0.98)(s+0.13)} \quad (1)$$

$$\frac{\delta \gamma}{\delta \theta_n} = \frac{31.3}{(s+0.5)(s+5.5)(s^2+5.45s+11.4)} \quad (2)$$

$$\frac{\delta \psi}{\delta \psi_n} = \frac{47}{(s^2+11s+58)(s^2+1.5s+0.81)} \quad (3)$$

where u = velocity, γ = flight-path angle, θ = pitch, and ψ = heading. The letter δ is used to identify the inputs as perturbations rather than commands and the outputs are the responses to these perturbations. The subscript n is used because the input perturbations are modeled as zero-mean

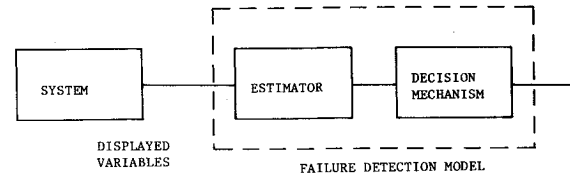


Fig. 1 Schematic block diagram.

white Gaussian processes. The source of these perturbations is usually the wind gusts, and therefore, the inputs to the subsystem are correlated and are derived from the amplitude and direction of the gusts.

Two of the preceding subsystems are of fourth order and one is of third order. Another integration of each subsystem output is needed to obtain the aircraft position. It is assumed that the pilot used only the dominant poles, namely the ones with the longer time constants. The final structure that is assumed for the pilot internal model is

$$\frac{\delta u}{\delta u_n} = 1/(s+1) \quad (4)$$

$$\frac{\delta \gamma}{\delta \theta_n} = 1.35/[(s+0.5)(s+2.7)] \quad (5)$$

$$\frac{\delta \psi}{\delta \psi_n} = 0.81/(s^2+1.5s+0.81) \quad (6)$$

The steady-state gain and the steady-state variance of the response to a stationary random input have been preserved as in the original system.

Having three decoupled system, eight state variables are defined by transforming Eqs. (4) to (6) to their state space format. Define

$$\begin{aligned} x_1 &= \delta u & x_2 &= \delta u & x_3 &= \delta \gamma & x_4 &= \delta \gamma \\ x_5 &= 0.585 \delta \alpha & x_6 &= \delta \psi & x_7 &= \delta \psi & x_8 &= g \delta \phi / v_0 \end{aligned} \quad (7)$$

where ϕ is the roll angle, α is the angle of attack, and g is acceleration due to gravity. The system dynamics in matrix notation are given by

$$\dot{\underline{x}} = \underline{F}\underline{x} + \underline{G}\underline{u} \quad (8)$$

where

$$\underline{F} = \begin{bmatrix} F_1 & 0 & 0 \\ 0 & F_2 & 0 \\ 0 & 0 & F_3 \end{bmatrix} \quad F_1 = \begin{bmatrix} 0 & 1 \\ 0 & 1 \end{bmatrix}$$

$$F_2 = \begin{bmatrix} 0 & 1 & 0 \\ 0 & 0 & 1 \\ 0 & -1.35 & -3.2 \end{bmatrix}$$

$$F_3 = \begin{bmatrix} 0 & 1 & 0 \\ 0 & 0 & 1 \\ 0 & -0.81 & -1.5 \end{bmatrix}$$

$$\underline{u}^T = [\delta u_n, \delta \theta_n, \delta \psi_n]$$

$$\underline{G}^T = \begin{bmatrix} 0 & 1 & 0 & 0 & 0 & 0 & 0 & 0 \\ 0 & 0 & 0 & 0 & 1.35 & 0 & 0 & 0 \\ 0 & 0 & 0 & 0 & 0 & 0 & 0 & .81 \end{bmatrix}$$

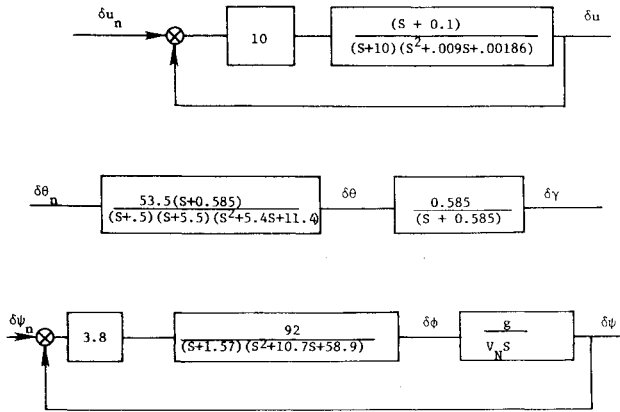


Fig. 2 Block diagrams of the three control loops.

The perturbations in the aircraft position in terms of the preceding state variables are given by (using the fact that γ_0 is small)

$$\delta x = \cos \psi_0 x_1 - v_0 \sin \psi_0 x_6 \quad (9a)$$

$$\delta y = \sin \psi_0 x_1 - v_0 \cos \psi_0 x_6 \quad (9b)$$

$$\delta x = \gamma_0 x_1 + v_0 x_3 \quad (9c)$$

where the subscripts 0 designate nominal values.

All the variables that are displayed to the pilot can now be represented as linear functions of the state variables.

1) Glideslope indicator

$$y_1 = (-\cos \psi_0 / x_N^2 + \gamma_0 / x_N) x_1 + v_0 x_3 / x_N + v_0 \sin \psi_0 x_6 / x_N^2$$

2) Localizer

$$y_2 = (\cos \psi_0 / (1.23 - x_N)^2 + \sin \psi_0 / (1.23 - x_N)) x_1 + (v_0 \cos \psi_0 / (1.23 - x_N) - v_0 \sin \psi_0 / (1.23 - x_N)^2) x_6$$

3) Airspeed indicator

$$y_3 = x_2$$

4) Attitude indicator

$$y_4 = x_4 + x_5 / 0.585 \quad (\text{pitch})$$

$$y_5 = v_0 x_8 / g \quad (\text{roll angle})$$

5) Horizontal situation display

$$y_6 = x_7$$

6) Altimeter

$$y_7 = \gamma_0 x_1 + v_0 x_3$$

7) Vertical speed indicator

$$y_8 = \gamma_0 x_2 + v_0 x_4$$

The variable x_N in these equations is the normal distance from touchdown which is time varying.

The Failure Detection Model

The Estimator

In the previous section, a simplified linear structure was discussed and was assumed to be used by the pilot as a model

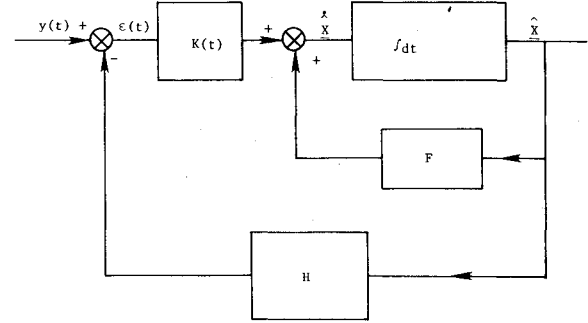


Fig. 3 Linear estimator (Kalman filter).

for the instrument output dynamics. The failure detection model suggested by Gai and Curry⁸ incorporates these simplified dynamics. The model consists of two stages: a linear estimator and a decision mechanism. The linear estimator, the Kalman filter, is shown in Fig. 3. It should be noted that the Kalman gain $K(t)$ is time varying due to the time-varying gains in the measurements. The filter produces estimates for the state $\hat{x}(t)$ and the measurements $\hat{y}(t)$ as well as the measurement error (residual) $\epsilon(t)$ defined as

$$\epsilon(t) = y(t) - \hat{y}(t) \quad (10)$$

Any of these three quantities can be used as input to the decision mechanism. The observation residual is preferred for the following reasons:

1) The state variables are nonunique variables that can be defined in many ways, while the observation residual is unique and well-defined for the observer.

2) The dimension of the state is in general larger than the dimension of the residual.

3) The residual is more sensitive than the observation to the effect of the failure.¹¹

4) The residual is a zero-mean white process¹² in the unfailed mode, so successive observations are independent for Gaussian processes.

Equation (10) implies the use of a scalar observation by the subject, even though there is some evidence that an independent rate measurement gives a better fit to the data when modeling the manual control tasks.³ However, since such an improvement was not found in the failure detection task,⁸ only direct (position) measurements were used.

Since the pilot is using more than one instrument, the problem of sharing of attention must be accounted for. This is done through the measurement noise in the observer model.¹³ When the pilot is monitoring only one instrument, the variance of his observation noise is proportional to the variance of the displayed signal (1/100 in Ref. 13). If the pilot is observing more than one instrument, the single-instrument variance of the observation noise for each observation is increased by a constant factor that is inversely proportional to the fraction of attention that he spends monitoring that specific instrument. Finally, it should be noted that although the state equations are decoupled, the Kalman filter is a coupled 8-dimensional system because of the coupling through the measurements. The model of the estimation scheme is shown in Fig. 4 (for three instruments).

The Decision Mechanism

The decision mechanism is based on sequential analysis.⁷ The classical sequential analysis uses the likelihood ratio $l(m)$ as a decision function after m observations. Two criteria levels, A and B , are chosen, and the decision rule is

if $l(m) \geq A$ choose "failure"

if $l(m) \leq B$ choose "normal"

if $B < l(m) < A$ take another observation

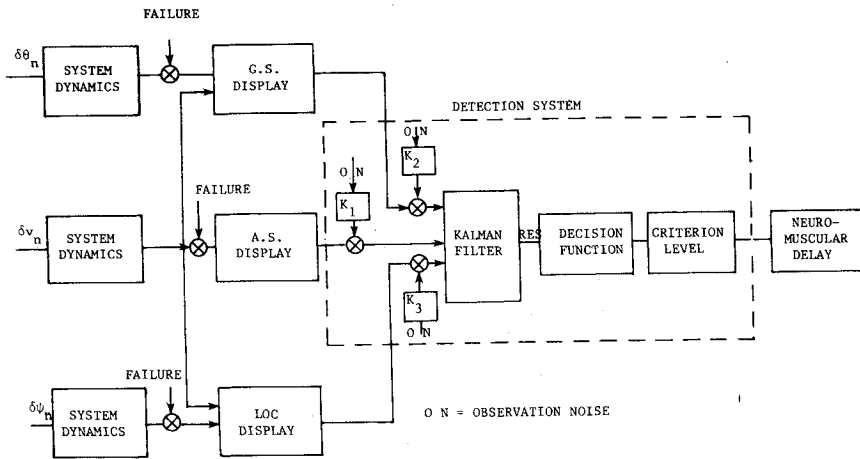


Fig. 4 Functional diagram of failure detection during automatic landing.

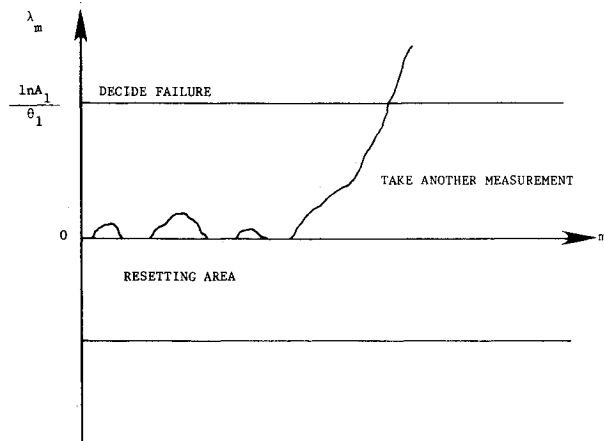


Fig. 5 Modified decision function.

A and B are determined by the desired probability of false alarm $P(FA)$ and the probability of miss $P(MS)$ as follows.⁷

$$A = (1 - P(MS)) / P(FA) \quad B = P(MS) / (1 - P(FA)) \quad (11)$$

In the current paradigm, we wish to treat the composite hypothesis

$$H_0: -\theta_l \geq \theta_0 = \bar{\epsilon}(t) \geq \theta_l \quad (12)$$

i.e., that the mean of the residual lies within a specified band of zero. Under suitable conditions,¹⁴ the most important of which is a monotonic likelihood ratio, a Uniformly Most Powerful test exists so that a test designed for the hypothesis (say) $\theta = \theta_l$ will also be adequate for $\theta \geq \theta_l$. Since in our case, both distributions are white Gaussian with equal variances and means zero and θ_l (failure), the decision function (for $\theta_l > 0$) is⁸

$$\tilde{\lambda}(m) = \sum_{i=1}^m \{\epsilon_i - \theta_l/2\} \quad (13)$$

The upper and lower criterion levels are

$$\ln A / \theta_l \quad (\text{upper}) \quad (14a)$$

$$\ln B / \theta_l \quad (\text{lower}) \quad (14b)$$

The classical theory cannot be directly applied to the failure detection problem because a basic assumption is that the same mode exists during the entire period. A failure detection problem is characterized by a transition from the normal mode to the failure mode at some random time t_f . In order to

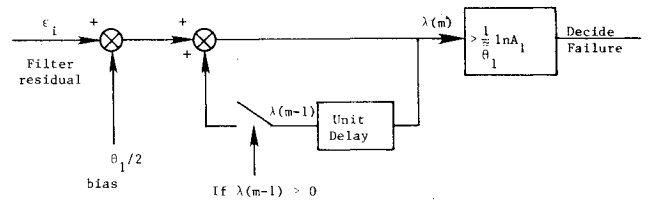


Fig. 6 Decision mechanism.

overcome this difficulty, the following modifications should be made:¹⁵

- 1) Resetting the decision function to zero whenever $\tilde{\lambda}(m)$ is negative, i.e., discounting confirmation of normal operation.
- 2) Using only an upper criterion level A_l which is modified to keep the same mean time between two false alarms as before.

The value of A_l is related to A and B in Eq. (11) by the equation

$$A_l - \ln A_l - I = -(\ln A + (A - I) \ln B / (I - B)) \quad (15)$$

The modified decision function is shown in Fig. 5 and the block diagram of the basic decision mechanism is shown in Fig. 6. For the case $\theta_l < 0$, the decision function is

$$\tilde{\lambda}(m) = \sum_{i=1}^m (\epsilon_i + \theta_l/2) \quad (16)$$

and only the lower criterion level is used. This criterion level is

$$-(\ln A_l) / \theta_l$$

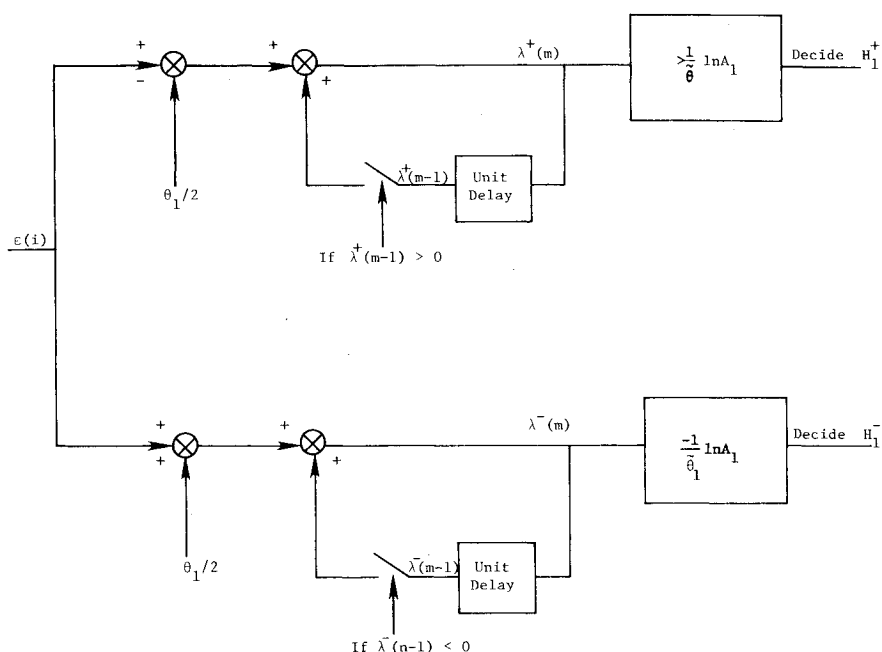
The final block diagram of the decision mechanism is shown in Fig. 7.

The operation of the proposed model is actually quite simple in principle. Its basic properties are:

- 1) A high-pass filter as a first stage to obtain the residuals.
- 2) Integration of the residual and comparison to a fixed threshold as a decision mechanism.⁸
- 3) Only three parameters control the performance of the model. a) The parameter designating the maximal mean of the observation error that is allowed before the system is considered "failed." b) The signal-to-noise ratio (SNR) of the observation. c) The probabilities of the two types of errors $P(FA)$ and $P(MS)$.

In the derivation of the decision rule in the preceding, it has been assumed that the observer uses an internal representation of the failure which is a constant bias of the mean (θ_l). Such a procedure is optimal for a step change in the mean, yet experimental results in Ref. 8 suggest that the observer uses a similar decision rule for detecting other types of changes, specifically a linear (ramp) change in the mean. Thus in what

Fig. 7 Complete block diagram of the decision mechanism.



follows we will assume that the observer uses the same decision rule regardless of the dynamic character of the additive failure.

The sensitivity of the model to changes in the various parameters was investigated in Ref. 8: it was found that the signal-to-noise ratio did not significantly alter the predictions of the model, whereas the detection performance $[P(FA), P(MS)]$ and the mean of the "failed" process (θ_1) were influential in the predictions. These parameters are not completely free, however, since they determine the decision criterion level through Eqs. (11), (14), (15), and (16).

Experimental Validation

The Adage Model 30 Graphics computer was used to simulate the nonlinear dynamics of a Boeing 707 and the control loops,⁹ and the output variables were drawn on a CRT instrument panel in the fixed-base simulator. The simulation included the last 5 min of flight starting at 10 miles from runway threshold at 2500-ft altitude with fully automatic approach and landing. The failures were instrument failures, so that they affected only the output variables and were not fed back to the system. In order to limit the experimental requirements, we considered only

failure in two instruments, the glidescope (GS) indicator and the airspeed (AS) indicator. Four levels of failures were included for each of the two instruments. All failures were step changes that were fed into the instrument through a single-pole low-pass filter with 10-sec time constant. The magnitude of the failure for the AS indicator were

$$c_1 = 2\sigma_v \quad c_2 = 3\sigma_v \quad c_3 = 4\sigma_v \quad c_4 = 5\sigma_v \quad (17)$$

and for the GS indicator

$$c_1 = \sigma_{GS} \quad c_2 = 1.5\sigma_{GS} \quad c_3 = 2\sigma_{GS} \quad c_4 = 2.5\sigma_{GS} \quad (18)$$

where σ_v and σ_{GS} are the standard deviations of the perturbations from the nominal of the displayed variable on the AS and GS indicators, respectively. Two random number generators were used to choose the failure in each run; one determined the instrument and the other the size of the failure. In addition, a third random number generator was used to determine the time of the failure t_f .

There was a single failure in 83% of the runs. The high percentage of runs with failures was chosen to provide enough data in a reasonable experimental time. It is evident that this

Table 1 Subjects and model performance parameters

Instrument	Statistical parameter	Failure magnitude	C_1	C_2	C_3	C_4
		Observer				
Airspeed	Mean detection time (seconds)	B.M.	20.8	13.8	10.8	6.3
		C.C.	25.4	20.8	16.9	8.2
		Model	22.8	13.3	9.5	6.8
Indicator	Standard error of the mean (seconds)	B.M.	2.6	1.2	0.9	1.2
		C.C.	2.6	1.8	1.1	1.2
		Model	2.0	1.3	0.9	0.6
Glidescope	Mean detection time (seconds)	B.M.	16.4	9.8	7.7	5.9
		C.C.	14.0	6.9	6.3	5.0
		Model	14.5	10.9	9.0	5.8
Indicator	Standard error of the mean (seconds)	B.M.	1.6	2.2	1.1	0.5
		C.C.	1.3	0.5	0.4	0.4
		Model	1.3	1.0	0.7	0.5

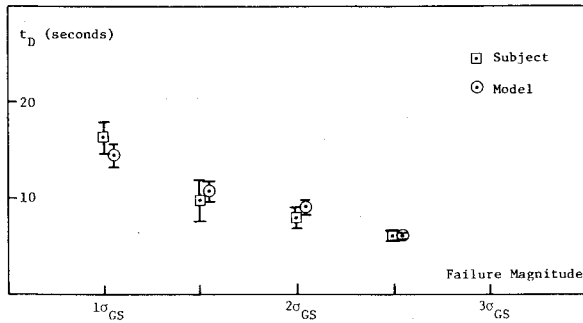


Fig. 8 Detection times for glidescope indicator failures (subject B.M.)

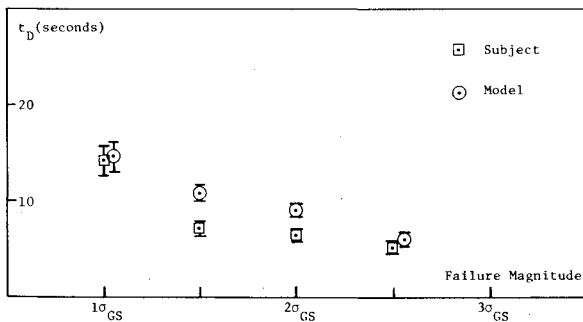


Fig. 9 Detection times for glidescope indicator failures (subject C.C.)

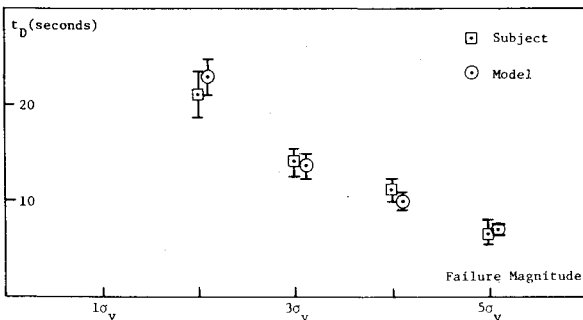


Fig. 10 Detection times for airspeed indicator failures (subject B.M.)

failure rate does not represent a realistic situation and might bias the subject to expect the failure. However, if a real-life failure rate had been used in repetitive runs, the vigilance of the observer might be severely affected. In order to account for this discrepancy when the model is used to predict real-life detection times, the bias term in the model can be modified to include the a priori probability of failure. Let P_f denote the a priori probability of failure, then the bias term $\theta_1/2$ in Eqs. (13) and (16) and in Figs. 6 and 7 should be replaced by

$$(\theta_1/2) - (1/\theta_1) \ln[P_f/(1-P_f)] \quad (19)$$

There was no feedback to the pilot concerning his performance because it was found that such feedback biased his decision, either by driving him to try to compensate for previous errors, or to overrelax after several correct decisions.

Each subject participated in three experimental sessions each of which included 16 runs for a total of 48 runs. When the pilot detected a failure, he pressed a button and the run was terminated. Otherwise, the run lasted until touchdown. After termination of each run, the subject was asked to fill out a form in which he stated which instrument failed and how he detected the failure.

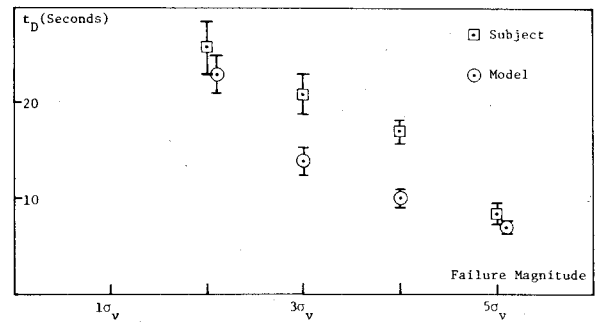


Fig. 11 Detection times for airspeed indicator failures (subject C.C.)

At the beginning of each session, a set of instructions was read to the subject. In particular, he was told that failure would be either in the AS or GS indicator, but that he could (and should) use other instruments for verification.

Results

The experimental results for two subjects (B.M. and C.C.) are summarized in Table 1. The table shows the mean detection time and the standard error of the mean (based on 5 samples) for each subject and for each of the two instruments. The table also includes the prediction of the model for the mean detection time and the error of the mean. These values were obtained by the use of a Monte Carlo simulation of the model using the same random processes as viewed by the subjects in the experiment. The values of three parameters that are needed for the model were chosen as follows.

$$\text{SNR} = 36 \quad P(FA) = P(MS) = 0.05 \quad \theta_1 = 0.25\sigma_{OB} \quad (20)$$

The signal to noise ratio is smaller by 4.5 dB from the one used in Ref. 13, however sensitivity studies⁸ show that the model is only slightly sensitive to SNR due to the good performance of the estimator. The observation error threshold θ_1 was chosen as one quarter of the observation standard deviation based on previous experimentation with the basic model.⁸ The values for $P(FA)$ were determined using the actual false alarm rate that was found in the experimental data.

The experimental results and the model prediction are also shown for each subject and each instrument in Figs. 8 through 11. Model predictions were slightly shifted to the right to prevent overlapping.

Conclusions

In this paper, a model is proposed for the performance of a pilot as a failure detector of instrument failures (additive dynamic biases) during an automatic landing. The model consists of two stages: a linear estimator and a decision mechanism. The linear estimator is the Kalman filter determined from a simplified model of displayed-variable dynamics used by the pilot. The filter also accounts for the pilot's time sharing between instruments through increased noise. The decision mechanism is based on classical sequential analysis with modifications for the failure detection case.

An experiment designed to test the validity of the model was conducted. In this experiment, subjects had to detect failures in the glidescope and airspeed indicators during a simulated landing in a Boeing 707 fixed-base simulator. The results show that the predicted detection times fit the experimental data well. It should be recalled that the model has currently been verified for failures which can be modeled as changes in the mean; further development is required to model changes in standard deviation, bandwidth, etc.

The use of the model for predicting absolute values of detection times depends on the limited experience with subject behavior in this task. It was found in this experiment and those reported elsewhere,⁸ that observers prefer to operate at equal and relatively low-error rates ($P(FA) = P(MS) = 0.05$)

with a bias parameter (θ_1) between one sixth to one quarter of the observation standard deviation. Will these values obtain in a realistic setting? Obviously, experimentation using real-life a priori probabilities and failure rates requires a prohibitive effort: one practical approach to the resolution of this dilemma is to first develop models of the human detection mechanism and then test the model validity and the changes of the parameters as more realistic situations are simulated. (The previous work in vigilance¹⁶ may be of some help in this regard.) Even at this stage, however, the model predictions may be explored by varying the parameters and determining whether or not uncertain parameter values are critical.

Acknowledgment

This work was sponsored by NASA Grant NGR 22-009-733, Man Machine Integration Branch, NASA Ames Research Center.

References

- ¹McRuer, D. T. and Jex, H. R., "A Review of Quasilinear Pilot Models," *IEEE Transactions on Human Factors in Electronics*, Vol. HFE-8, Sept. 1967, pp. 231-249.
- ²McRuer, D. T. and Krendel, E.S., "Mathematical Models of Human Pilot Behavior," AGARD Rep. #188, July 1974.
- ³Kleinman, D. L. and Baron, S., "Manned Vehicle Systems Analysis by Means of Modern Control Theory," NASA Rep. CR-1753, June 1971.
- ⁴Sheridan, T. B. and Ferrel, W. R., *Man Machine Systems*, MIT Press, Cambridge, Mass., 1974.
- ⁵Phatak, A. V. and Kleinman, D. L., "Current Status of Models for the Human Operator as a Controller and Decision Maker in Manned Aerospace Systems," Proceedings of the AGARD Conference, #114, Oct., 1972, pp. 16.1-16.10.
- ⁶Clement, W. F., McRuer, D. T. and Klein, R., "Systematic Manual Control Display Design," Guidance and Control Displays, AGARD CP-96, Oct., 1971.
- ⁷Wald, A., *Sequential Analysis*, Wiley, New York, 1947.
- ⁸Gai, E. G. and Currey, R. E., "A Model of the Human Observer in Failure Detection Tasks," *IEEE Transactions on Systems, Man, and Cybernetics*, Vol. SMC-6, Feb. 1976, pp. 85-94.
- ⁹Ephrath, A. R., "Pilot Performance in Zero Visibility Precision Approach," Ph.D. Thesis, Department of Aeronautics and Astronautics, Massachusetts Institute of Technology, Cambridge, Mass., June 1975.
- ¹⁰Blacklock, J. H., *Automatic Control of Aircraft and Missiles*, Wiley, New York, 1965.
- ¹¹Schweppe, F.C., *Uncertain Dynamic Systems*, Prentice Hall, Englewood Cliffs, N.J., 1973.
- ¹²Kailath, T., "The Innovation Approach to Detection and Estimation Theory," *Proceedings of the IEEE*, Vol. 58, May 1970, pp. 680-695.
- ¹³Levison, W. H., "A Control Theory Model for Human Decision Making," Proceedings of the Seventh Annual Conference on Manual Control, 1971.
- ¹⁴Rao, C. R., *Linear Statistical Inference and its Applications*, Wiley, New York, 1973.
- ¹⁵Chien, T. T., "An Adaptive Technique for a Redundant Sensor Navigation System," C. S. Draper Laboratory Rep. T-560, 1972.
- ¹⁶Mackworth, J. F., *Vigilance and Habituation*, Penguin Science of Behavior, New York, 1969.

From the AIAA Progress in Astronautics and Aeronautics Series

AERODYNAMICS OF BASE COMBUSTION—v. 40

*Edited by S.N.B. Murthy and J.R. Osborn, Purdue University,
A.W. Barrows and J.R. Ward, Ballistics Research Laboratories*

It is generally the objective of the designer of a moving vehicle to reduce the base drag—that is, to raise the base pressure to a value as close as possible to the freestream pressure. The most direct and obvious method of achieving this is to shape the body appropriately—for example, through boattailing or by introducing attachments. However, it is not feasible in all cases to make such geometrical changes, and then one may consider the possibility of injecting a fluid into the base region to raise the base pressure. This book is especially devoted to a study of the various aspects of base flow control through injection and combustion in the base region.

The determination of an optimal scheme of injection and combustion for reducing base drag requires an examination of the total flowfield, including the effects of Reynolds number and Mach number, and requires also a knowledge of the burning characteristics of the fuels that may be used for this purpose. The location of injection is also an important parameter, especially when there is combustion. There is engineering interest both in injection through the base and injection upstream of the base corner. Combustion upstream of the base corner is commonly referred to as external combustion. This book deals with both base and external combustion under small and large injection conditions.

The problem of base pressure control through the use of a properly placed combustion source requires background knowledge of both the fluid mechanics of wakes and base flows and the combustion characteristics of high-energy fuels such as powdered metals. The first paper in this volume is an extensive review of the fluid-mechanical literature on wakes and base flows, which may serve as a guide to the reader in his study of this aspect of the base pressure control problem.

522 pp., 6x9, illus. \$19.00 Mem. \$35.00 List

TO ORDER WRITE: Publications Dept., AIAA, 1290 Avenue of the Americas, New York, N. Y. 10019